Decreased expression of profilin 2 in oral squamous cell carcinoma and its clinicopathological implications

C.Y. MA[1,2], C.P. ZHANG[1,2], L.P. ZHONG[1,2], H.Y. PAN[1,2], W.T. CHEN[1,2], L.Z. WANG[3], O.W. ANDREW[4], T. JI[1] and W. HAN[1,2]

[1]Department of Oral and Maxillofacial Surgery, Ninth People's Hospital, College of Stomatology; [2]Shanghai Key Laboratory of Stomatology and Shanghai Research Institute of Stomatology; [3]Department of Oral Pathology, Ninth People's Hospital, College of Stomatology, Shanghai Jiao Tong University School of Medicine, Shanghai 200011, P.R. China; [4]Department of Oral and Maxillofacial Surgery, Faculty of Dentistry, National University of Singapore, Singapore 119074, Singapore

Received February 8, 2011; Accepted April 11, 2011

DOI: 10.3892/or.2011.1365

Abstract. Profilins are small proteins essential for many normal cellular dynamics and constitute one of the crucial components of actin-based cellular motility. Several recent studies have implicated a role for the profilin (PFN) family in cancer pathogenesis and progression. However, their expression and promising functions are largely unknown in oral squamous cell carcinoma (OSCC). In this study, we analyzed the correlation between PFN1 and PFN2 expression *in vitro* and *in vivo*. The protein expression levels were roughly compared between cell lines (HIOEC, HB96) with the employment of mass spectrometry. PFN2 was singled out as one of the significantly down-regulated genes in the cancerous HB96 cells. The expression levels of PFN1 and PFN2 *in vitro* were validated by RT-PCR, real-time PCR and Western blotting. Laser scanning confocal microscopy was used for the first time to assess the localization of PFN2 expression. In subsequent experiments, we observed the relationship between PFN2 expression levels and the proliferation of transfected HB96 cancer cells. VASP, N-WASP and P27 expression was also examined in the PFN2-transfected or non-transfected HB96 cells. *In vivo*, antigen expression was determined by immunohistochemical analyses in 88 paired tissue specimens. Decreased protein expression was confirmed in cancerous tissues from 88 OSCC patients compared with paracancerous normal mucous epithelia. Tumors with weak PFN2 expression were associated with a significantly worse prognosis than strongly expressed tumours (P<0.001). Other statistical analyses were performed to assess the differences in expression and their clinical and pathological significance. In conclusion, PFN2 can be utilized as both a potential suppressor marker and a prognostic protein for OSCC. The function of PFN2 may be to regulate the N-WASP/Arp2/3 signaling pathway.

Correspondence to: Dr Chen-Ping Zhang, Department of Oral and Maxillofacial Surgery, Ninth People's Hospital, College of Stomatology, Shanghai Jiao Tong University School of Medicine, Shanghai 200011, P.R. China
E-mail: h9mfsl@online.sh.cn

Key words: profilin, decreased expression, oral squamous cell carcinoma, prognosis, N-WASP

Introduction

Oral squamous cell carcinoma (OSCC) is a significant public health problem with >300,000 new cases being diagnosed annually worldwide (1). The prognosis of OSCC remains relatively unfavorable, with the overall survival rate at 5 years oscillating between 40 and 55% (2,3). Further, it has been observed that ~40% of OSCC patients die from uncontrolled locoregional disease alone, and 24% show metastases to distant sites, even though more radical therapies have now been applied (4). Given the malignant nature of the disease, early detection and more effective therapies are urgently needed (5). However, a poor understanding of the biology of the disease, imperfect screening of biomarkers and the presence of only a few symptoms or warning signs in early-stage disease all contribute to treatment failure (6).

Recent efforts have been focused on the discovery of particular biomarkers that can distinguish between the specific biological properties of normal and cancer cells (7). The extraordinary developments made in proteomic technologies in the past decade have enabled investigators to search for biomarkers by simply scanning through proteomic data (8). Perhaps the most well-known method of comparing protein abundances within complex proteomes is the combination of two-dimensional polyacrylamide gel electrophoresis (2-D PAGE) fractionation with mass spectrometry (MS) protein identification (9,10). The wide application of this technique in studies of different types of solid tumors, such as breast (11), lung (12), colorectal (13) and liver cancer (14), has spurred the same fervor in the unveiling of specific epithelial biomarkers of OSCC. The advent of proteomic technologies allowing high-throughput and unambiguous identification of proteins have made it possible to undertake the present study.

Profilins (PFNs) are small proteins (12-15 kDa) that were originally considered to bind ATP-actin monomers with high

affinity and catalyze nucleotide exchange (ATP for ADP) on actin filaments, which comprise a major part of the cytoskeleton (15,16). This ATP-hydrolysis-driven, directional actin-filament growth is called treadmilling, and is the driving force behind cell locomotion, morphogenetic movements and many cellular transport events (17,18). PFN1 and PFN2, represent the first two isoforms of the PFN family, which has been discovered for several years. PFN1 was claimed to be ubiquitously expressed except in skeletal muscle and actively involved in the regulation and reorganization of the cytoskeleton and non-muscle cell motility (19). Most of the research on PFN2 involves its functions on neurotransmitter exocytosis in glutamatergic neurons (20). Recently, the potential of the PFN family in reducing tumor progression and a role in regulating the Akt/PTEN signaling pathway has been suggested. (21) While PFN1 has been demonstrated to act as a tumor suppressor, the role of the PFN family in OSCC has not yet been elucidated. In this study, we first identified the decrease of PFN1 and PFN2 mRNA expression in several OSCC cell lines compared with the human immortalized oral epithelial cells (HIOECs). We further investigated the significance of the PFN2 down-regulation and its potential usefulness as a clinical, pathological or prognositic marker for OSCC.

Materials and methods

Sample collection and patient follow-up. Pathological tissue samples were retrieved from the Department of Oral Pathology Shanghai Ninth People's Hospital, School of Medicine, Shanghai Jiao Tong University, after approval by the Ethics Committee of Biomedical Research in the Shanghai Ninth People's Hospital. A total number of 88 patients with primary oral squamous carcinoma with no preoperative chemo- or radiotherapy were enrolled in this study. Written informed consent was obtained before the treatment. After signing the informed consent forms, they all underwent surgery at the Department of Oral and Maxillofacial Surgery of Shanghai Ninth People's Hospital between Febuary 2007 and December 2008. Ten percent buffered formalin-fixed and paraffin-embedded tissues were used for immunohistochemical examination. Histological diagnosis was established on the basis of standard hematoxylin and eosin-stained sections of each sample. The pathological types of cancer were classified according to the 2005 WHO guidelines. The tumor node metastasis (TNM) staging was conducted according to the 2009 UICC staging system. All these patients received surgery with a curative intention. All patients were followed up till death or December 2010.

Cell cultures. Our previous research established a stable cell line of HIOECs, which are fundamentally close to the properties of normal oral mucosa, with the transfection of HPV16 E6/E7 gene (22), and then subsequently derived it into a cancerous cell line (HB96) by treatment with benzo[a]pyerene for 6 months (23). These two types of cells constituted the major components of the *in vitro* cellular carcinogenesis model of OSCC in our lab. The biological characteristics of HIOEC HB96 have been previously described including cell morphology, cell ultrastructure, cell growth, cell cycle analysis, immunocytochemistry, *in vitro* invasion ability and tumorigenicity (24). The Tca8113 cell line was derived from human tongue carcinoma (25). The oral cancer cell lines OSC and NT were provided by Kochi Medical School, Japan as a gift. CAL27 cells were purchased from the American Type Culture Collection (Manassas, VA). HIOECs were cultured in the defined keratinocyte-SFM (Gibco, USA). HB96, CAL27, Tca8113 cells were cultured in DMEM (Gibco). OSC, NT cells were cultured in the RPMI-1640 (Invitrogen, CA). These cancer cells were supplemented with 10% fetal bovine serum, 1% glutamine and 1% penicillin-streptomycin.

Two-dimensional gel electrophoresis (2-DE) and liquid chromatography-tandem mass chromatography (LC-MS/MS). HIOEC and HB96 cells at 80% confluency were lysed in 300 μl ice-cold lysis buffer containing 8 M Urea, 65 mM DTT, 4% (w/v) CHAPS, 40 mM Tris, and freshly prepared 100 μg/ml PMSF. Cells were then sonicated 10 times (15 sec each) and centrifuged at 12,000 x g for 90 min. The concentration of the crude proteins in the supernatant was determined using the Bradford protein assay reagent (Bio-Rad protein Dye assay reagent; Bio-Rad, Hercules, CA, USA). The 17-cm pH 3-10 immobilized pH gradient (IPG) strips (Bio-Rad, cat. no. 163-2009) were first rehydrated in sample buffer at 17˚C, and then subjected to isoelectric focusing (IEF) following the manufacturer's instructions (Bio-Rad) with modifications. IEF was run at 250 V for 30 min at linear mode, followed by 1,000 V for 60 min at rapid mode, 10,000 V for 5 h at linear mode, 10,000 V for 6 h at rapid mode, and 500 V at linear mode. After IEF, strips were equilibrated for 2x15 min at room temperature in equilibration buffer (6 M urea, 30% glycerin, 2% SDS, 375 mM Tris-HCl pH 8.8), first supplemented with 2% DTT and then with 2.5% iodoacetamide to replace DTT. Equilibrated IPG strips were then transferred onto 12% uniform polyacrylamide gels, and the second dimensional gel separation was performed with a Hoefer SE600 Ruby system (Amersham Biosciences, Sweden). Constant 5 mA/gel current was applied, followed by 30 mA/gel until the bromophenol blue front reached the bottom of the gels. Two-dimensional standards were added to the protein samples as internal markers to determine the isoelectric point (pI) and molecular weight (M_r). The gels were stained by $AgNO_3$ for 20 min, and scanned by the Bio-Rad GS710 scanner (Bio-Rad). Spot detection and matching were performed using PDQuest software version 7.3.0 (Bio-Rad). The analytic gel images were normalized according to the total protein quantity. Relative spot intensities among protein samples from three cells were compared using Student's t-test. All samples were applied as triplicates at three time points from each cell line. Differences in spot intensities >5.0-fold ($P<0.05$) or <0.2-fold ($P<0.05$) were set as a threshold values indicating significant changes of protein expression.

Following the automated protein localization and quantification, gel spots carrying the proteins were excised by a spot cutter (Bio-Rad) controlled by the PDQuest software. Excised gels were then triturated, the proteins were washed off with ammonium bicarbonate and acetonitrile, and digested by trypsin. The peptides in the solution were then dried by vacuum centrifugation, desalted and cleaned by a C18 Ziptip (Millipore, USA). Peptides were separated and detected by a Finnigan LTQ mass spectrometer coupled with a Surveyor

HPLC system (ThermoQuest, USA); MS/MS raw data were analyzed and the proteins were identified by the SEQUEST program in the BioWorks 3.1 software suite (University of Washington, licensed to Thermo Finnigan) based on the IPI Human database version 3.15.1.

RT-PCR and quantitative real-time RT-PCR. Total RNA was extracted from human OSCC cell lines at 80% confluence using TRIzol reagent (Invitrogen) according to the manufacturer's protocol and RNA was isolated and then synthesized into complementary DNA (cDNA) by using a PrimeScript RT reagent kit (Takara, Shiga, Japan).

Amplification of PFN1 cDNA was performed using the forward primer, 5'-CGAGTCTCGTGGGCTACAAGGAC TCG-3' and the reverse primer, 5'-CAACCAGGACACCCAC CTCAG-3', and the length of the PCR product was 220 bp. PCR amplification of PFN2 was performed using the forward primer, 5'-TGTCGGCAGAGCTGGTAGAGTCTT-3', the reverse primer, 5'-GCAGCTAGAACCCAGAGTCTCTC AA-3', and the length of the PCR product was 122 bp. The primer sequences of GAPDH used as an endogenous control were: forward primer, 5'-GGATTTGGTCGTATTGGG-3', and reverse primer 5'-GGAAGATGGTGATGGGATT-3'. The length of the GAPDH PCR product was 211 bp. Reverse-transcription PCR reactions were amplified for 32 cycles using the standardized conditions by adding 10 μl Premix Taq (Takara). The RT-PCR products were separated by 1.5% TAE agarose gel electrophoresis.

The real-time PCR analyses were performed using SYBR® Premix Ex Taq II (Takara). Sequences of PFN2 primers for real-time PCR were designed in the same manner as in RT-PCR. Real-time PCR was performed with a Takara PCR Thermal Cycler Dice Detection system and SYBR-Green dye (Takara). The relative quantification of PFN2 mRNA level to the mRNA level of GAPDH was assessed according to the $2^{-\Delta\Delta Ct}$ method.

Western blotting. Cultured cells were treated with CelLytic™ MEM protein extraction kit (Sigma-Aldrich, USA), NE-PER® nuclear and cytoplasmic extraction reagents (Pierce, USA) adding 10 μl/ml phosphatase inhibitor cocktail I and II (Sigma-Aldrich), and whole protein, nuclear (NEs) and cytosolic extracts (CEs) were obtained according to standard procedures. The lysates were separated by 12% SDS-polyacrylamide gel electrophoresis, subsequently transferred to polyvinylidene difluoride (PVDF) membranes (Bio-Rad) in a wet system. The membranes were blocked with blocking buffer containing 5% dry milk in pH 7.4 TBS (Tris-buffered saline) (Sangon, Shanghai) with 0.1% Tween-20 and incubated overnight with the following primary antibodies: mouse anti-PFN2 monoclonal (Abcam, UK) at 1:1,000 dilution; rabbit anti-PFN1 polyclonal (Abcam) at 1:1,500; rabbit anti-N-WASP or anti-P27 polyclonal (Abcam) at 1:1,000; rabbit anti-VASP ploYclonal (Santa Cruz Biotechnology, USA) 1:200; rabbit anti-histone H3.1 polyclonal 1:500 (Signalway, USA); mouse anti-GAPDH monoclonal or rabbit anti-GAPDH polyclonal antibody (Abcam) at 1:5,000. The blot was then incubated with horseradish peroxidase-conjugated anti-mouse or anti-goat IgG secondary antibody (KPL, USA). The membrane was treated with Supersignal West-Pico chemiluminescent substrate (Pierce) and exposed to Fuji X-ray film (Fuji, Japan).

Immunofluorescence microscopy. After the treatment, the HIOEC, HB96, CAL27 cells were fixed (4% formaldehyde in PBS), the plasma membrane was permeabilized (Triton X-100, 0.1%), and microfilaments were labelled with phalloidin–TRITC (tetramethylrhodamine β-isothiocyanate) for 20 min. All cells were incubated with PFN2 antibody at 1:500 dilution. After washing with PBS, the sections were stained with FITC (fluorescence isothiocyanate)-conjugated anti-mouse IgG (Molecular Probes). For staining of filamentous actin (F-actin), TRITC-conjugated phalloidin (Molecular Probes) was used. Nuclei were counterstained with DAPI (4',6-diamidino-2-phenylindole; Sigma). Immunofluorescent images of these cultured cells were observed by a laser scanning confocal microscope (Leica TCS SP2).

Construction of PFN2 expression vector. Full-length human PFN2 cDNA was amplified by RT-PCR using the forward primer 5'-GCGGCCGCatggccggttggcagagctacg-3', and the reverse primer 5'-GGATCCttacacatcagacctcctcag-3' based on the cDNA sequence of PFN2 (accession no. NM_002628.4). RT-PCR was performed by using SuperScript™ II reverse transcriptase (Invitrogen). The PCR product (453 bp), which contained the full coding region of PFN2 as confirmed by sequencing, was cloned into pCR-Blunt (Invitrogen). To construct the PFN2 expression vector, the PFN2 coding sequence was released from pCR-Blunt by *Not*I and *Bam*HI digestion and subcloned into the expression vector pQCXIH (Clontech, CA). The orientation of the gene in the vector was determined by restriction enzyme digestion and sequencing. The resultant PFN2 expression vector was designated pQCXIH-PFN2, in which PFN2 cDNA was driven by a mouse sarcoma virus (MSV) promoter and a cytomegalovirus (CMV) enhancer.

Plasmid transfection and MTT assay. To characterize the PFN2 expression vector, pQCXIH-PFN2 or empty vector pQCXIH, was transfected into HB96 cells using Lipofectamine™ 2000 (Invitrogen) following the manufacturer's instructions. Cells were seeded in a 6-well plate at $2x10^5$ cells per well 24 h prior to transfection when they were cultured to a confluency of ~80%. For Western blotting and cell count, HB96 cells were transfected with 1.5 μg of plasmid and 2.5 μl of Lipofectamine™ 2000 in 6-well plates. The MTT cell growth assays were used to determine the potential anti-proliferation effect of PFN2 on HB96 cancer cell growth. Cells were transfected with 60 ng of plasmid and 0.08 μl of Lipofectamine 2000 in 96-well plates. Cells were harvested and tested at 24, 48, 72 and 96 h after transfection. The MTT assay was carried out by adding MTT to a final concentration of 1 g/l in 96-well plates with a total of 5,000 cells per well and incubation in a 5% CO_2 incubator at 37˚C for 4 h. After supernatant was removed, the cells were added with 150 μl DMSO (Sigma) per well and cultivated for 30 min. Absorbance in each well was measured at 570 nm using a microplate reader (ELX800, Bio-Tek Instruments). Cell growth curves were measured on the corresponding values.

Immunohistochemical analysis. Paired cancerous and para-cancerous normal tissue samples from each of 88 patients were assayed for PFN2 using immunohistochemical staining. The procedure of immunohistochemistry was in accordance with a previously described method (26).

Microscopic examination was performed in a blinded fashion by two pathologists. The staining was evaluated by scoring the percentage of positive cancer or normal epithelial cells according to the following scale. The PFN2-positive grade was determined based on the the intensity of staining in both the nucleus and cytoplasm of stained cells on a scale of negative to strong as follows: 0, no staining; 1, weak staining; 2, moderate staining; and 3, strong staining. Tumours with an intensity score ≥2 were considered to have high expression of target protein in the correlation analysis.

Statistical analysis. All data was analyzed by the software SAS 9.2 for Windows (SAS Inc., USA). Survival curves were obtained by the Kaplan-Meier method. Overall survival of patients with low versus high PFN2 expression was analyzed using the log-rank test. Multivariable Cox proportional hazard regression analysis was performed with overall survival as the response variable. To verify the proportional hazards model assumption, we tested the hazard ratios for covariates changed with time (including age, gender, histological grade, PFN2 expression, primary tumor size, regional lymph node and clinical stage). P<0.05 was considered statistically significant.

Results

Patient characteristics. The study population consisted of 57 males and 31 females with a male-to-female ratio of ~2:1. The sites of primary carcinoma were tongue (n=46), buccal mucosa (n=21) floor of mouth (n=10), and gingiva (n=11). The duration of follow-up ranged from 2 to 45 months (median follow-up period: 22.5 months) (Table I). Of all the cases, 35 were categorized as well-differentiated squamous cell carcinoma, 40 moderately-differentiated and 13 poorly-differentiated.

2-DE and LC-MS/MS. We compared the protein expression profiles among HIOECs and HB96 cells by using 2-DE. With HIOEC being the negative control, we identified 26 different proteins from HIOECs and 19 proteins from HB96 cells. Among them, one protein was significantly down-regulated in HB96 cells as marked by the circles in Fig. 1A and was later verified by LC-MS/MS as PFN2. By searching the IPI Human database (version 3.15.1), their peptide fingerprint matched known peptides, as shown in Fig. 1B.

PFN1 and PFN2 expression at the mRNA level in normal and squamous carcinoma cell lines. To confirm these proteomic findings in the OSCC cell lines, we attempted to identify the specific expression of PFN1 and PFN2 mRNA *in vitro*. RT-PCR showed that the mRNA level of PFN2 was lower in most of the OSCC cell lines, including HB96, Tca8113, OSC, NT, CAL27 (Fig. 2A). Real-time PCR results also showed that the mRNA level of PFN2 was decreased in most cancerous cells compared with HIOEC (Fig. 2C). CAL27 had the most decreased amount of mRNA by 3-fold compared with the immortalized normal cell line HIOEC. However, there was no discernable difference in the mRNA expression in PFN1 between the 5 cancerous cells and HIOEC by RT-PCR analysis (Fig. 2A). The real-time PCR results of PFN1 were not prominent and the mRNA of PFN1 was expressed in roughly the same level by comparing all these cell lines (Fig. 2B).

Table I. Patient clinical and histopathological data and Kaplan-Meier survival analysis of the clinicopathological variables and PFN2 expression.

Variables	No. of cases (%)	P-value
No. of patients	88 (100)	
Age (years)		
≤60	52 (59.1)	0.140
>60	36 (40.9)	
Gender		
Male	57 (64.8)	0.766
Female	31 (35.2)	
Tumor site		
Tongue	46 (52.3)	0.261
Buccal mucosa	21 (23.7)	
Floor of mouth	10 (11.5)	
Gingiva	11 (12.5)	
Histological grade		0.004
Well-differentiated	35 (39.8)	
Moderately-differentiated	40 (45.4)	
Poorly-differentiated	13 (14.8)	
Vascular invasion		0.017
Yes	28 (31.8)	
No	60 (68.2)	
Tumor stage		0.013
Stages I+II	31 (35.2)	
Stages III+IV	57 (64.8)	
Tumor size		0.103
T1-2	50 (56.8)	
T3-4	38 (43.2)	
Regional lymph nodes		0.066
N0	37 (42.0)	
N1-3	51 (58.0)	
PFN2 expression		<0.001
None	25 (28.4)	
Weak	33 (37.5)	
Moderate	28 (31.8)	
Strong	2 (2.3)	

PFN1 and PFN2 expression at the protein level in a panel of OSCC cell lines by Western blotting. By Western blotting, specific bands for PFN1 and PFN2 were detected by using specific antibodies for the whole cell protein lysate. Western blot analysis revealed that the PFN2 protein expression level was decreased in HB96 cells as well as other OSCC cell lines Tca8113, NT, CAL27 when compared with the level in HIOECs upon normalization against GAPDH protein signals (Fig. 2D). PFN2 expression pattern by Western blotting was consistent with the finding obtained form the comparative proteomic analysis. What is more, these coincided with the findings at the mRNA level, demonstrating the decreased

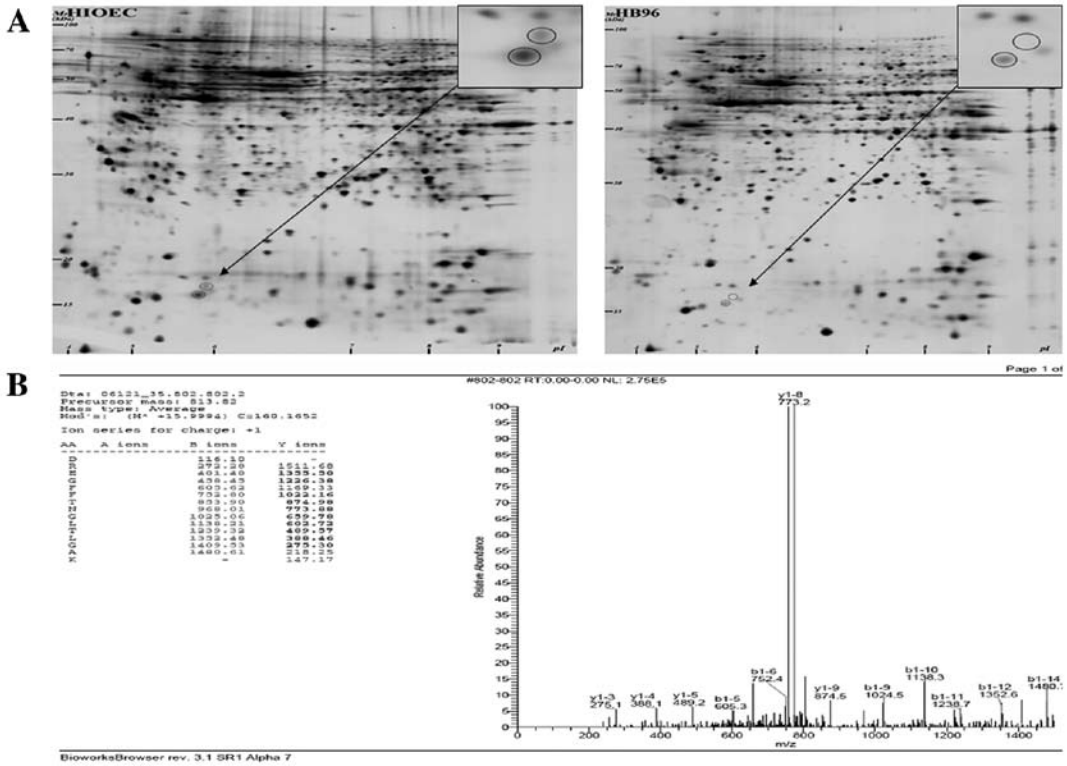

Figure 1. Two-dimensional gel electrophoresis (2-DE) map of the protein expression in HIOEC (as a control) and HB96 oral cancer cells. (A) The area enclosed by black circles in the two images indicates the differential expression of PFN2 which was successfully identified. (B) Peptides fingerprint of PFN2 marked and identified by LC-MS/MS.

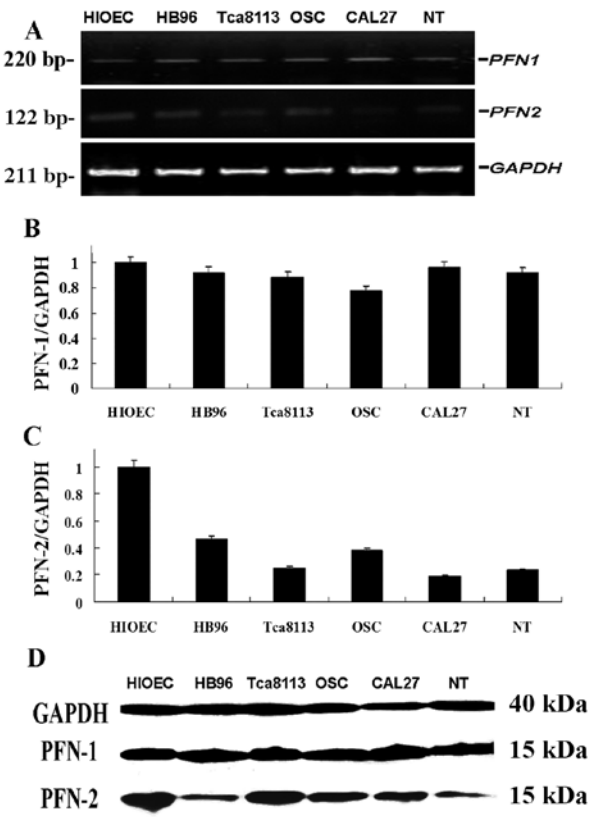

Figure 2. The expression of PFN2 in OSCC cell lines by RT-PCR, real-time PCR and Western blotting. (A) Decreased expression of PFN2 mRNA in HIOEC compared with HB96, Tca8113, OSC, CAL27 and NT cancer cell lines. (B and C) Real-time PCR demonstrated a decrease in the mRNA levels of PFN2 while no significant changes for PFN1. (D) Western blotting also revealed low expression of PFN2 in cancer cells *in vitro*.

PFN2 expression at both the mRNA and protein levels *in vitro*. These findings are also compatible with the results of immunostaining in pathological tissues for they show the same tendency for PFN2. On the other hand, the PFN1 protein expression in Western blotting showed no obvious difference between cancer and non-tumorigenic HIOEC cells. We therefore, chose to focus our subsequent *in vivo* experiments on PFN2 rather than on PFN1.

Subcellular localization of PFN2 in HIOEC, HB96 and CAL27 cell lines by immunofluorescence microscopy and Western blotting. There have been no reports on the subcellular expression of PFN2 in oral mucosal cells and tissues. Confocal microscopic images indicated that PFN2 localized on both cytoplasmic and nuclear regions of the cells (Fig. 3A-C). When comparing the PFN2 signal in the tumor cells HB96 and CAL27, PFN2 expression levels were lower in tumor cells especially in their cytoplasmic regions. To verify the observations in the confocal images, Western blot analysis of the subcellular proteins was performed in nuclear and cytoplasmic protein extracts as described in Materials and methods. Judging from the Western blotting results, while the nuclear PFN2 protein levels for normal and tumor cells remained almost the same, the expression of PFN2 in the cytoplasm differed. HIOECs expressed strong cytoplasmic signals of PFN2, while the PFN2 signal in CAL27 and HB96 was low to zero (Fig. 3D and E).

Inhibition of cell growth and expression of VASP, N-WASP and P27 after PFN2 transfection in HB96 cells. To determine if PFN2 plays a role in cell growth, we used pQCXIH-PFN2 vector to transiently overexpress PFN2 in OSCC cells with low

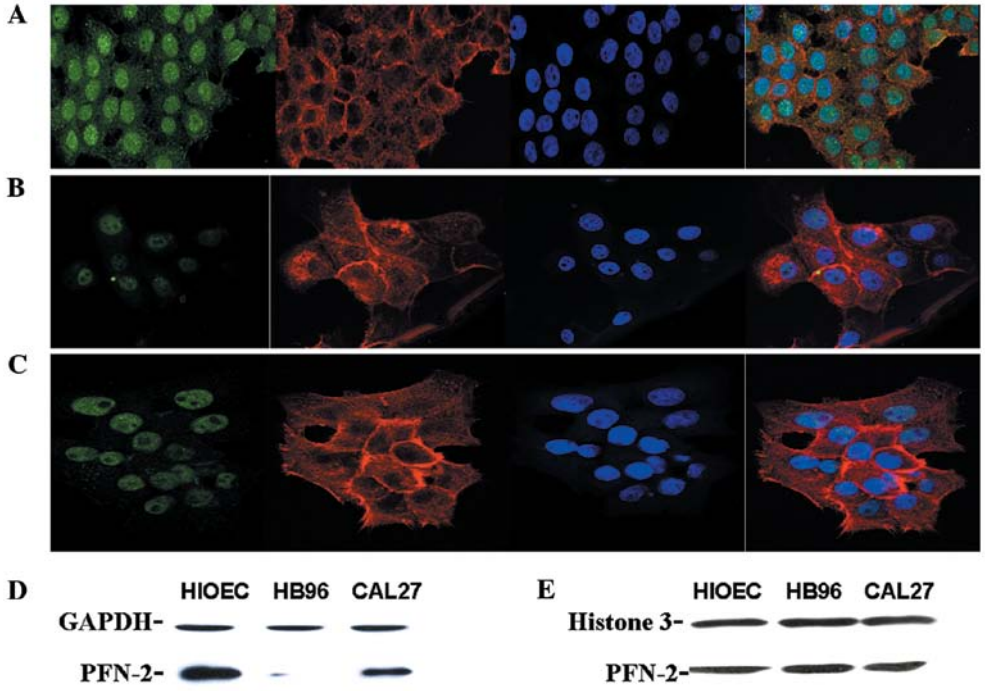

Figure 3. Confocal microscopy analysis of the subcellular localization of PFN2 *in vitro*. (A) Confocal images of PFN2 expression in HIOEC. The green signals depict the target protein PFN2, and the red the F-actin, while the blue shows nuclear staining. (B) Confocal images of PFN2 expression in HB96. (C) Confocal images of PFN2 expression in CAL27. (D) Decreased expression of cytoplasmic PFN2 in cancerous HB96 compared with normal HIOEC cells. (E) PFN2 expression in the nuleus remained almost the same among HIOEC, HB96 and CAL27.

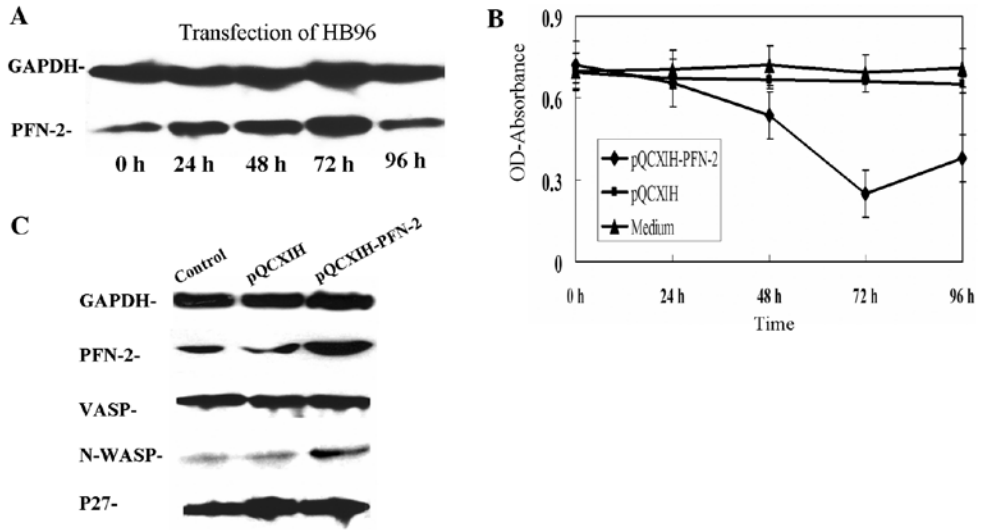

Figure 4. Transient transfection of HB96 with pQCXIH-PFN2 vector, MTT cell growth comparison and potenital downstream signaling pathway proteins. (A) HB96 cancerous cells were transfected with pQCXIH-PFN2 vector and the most evident change in protein levels could be obtained 72 h after the transfection. (B) The MTT assay of cell growth of HB96 with pQCXIH-PFN2 or empty pQCXIH vector, respectively, with non-transfected HB96 being the control group. (C) VASP, N-WASP and P27 were selected and no consequent change of expression could be seen in VASP and P27 while N-WASP increased after transfection of the PFN2 vector.

amounts of endogenous PFN2. Western blotting showed that PFN2 expression increased in the first 72 h (Fig. 4A). The MTT assay was used to evaluate the effect of PFN2 on OSCC cell growth. A dramatic decrease of cell growth was observed in HB96 cells with pQCXIH-PFN2 transfection compared with empty vector-transfected and non-transfected cancer cells (Fig. 4B).

The potential role of PFN2 as a negative regulator of OSCC growth and aggressiveness was further explored by examining the downstream molecular interaction between VASP, N-WASP or P27 and PFN2. As shown in Fig. 4C, the expression of N-WASP was increased by transfection of the pQCXIH-PFN2 vector, while those of VASP and P27 remained unchanged.

PFN2 protein expression in OSCC tissue samples and correlation with clinical and pathological characteristics. To further investigate the role of PFN2 *in vivo*, we performed immunohistochemistry on paraffin sections of the 88 patients.

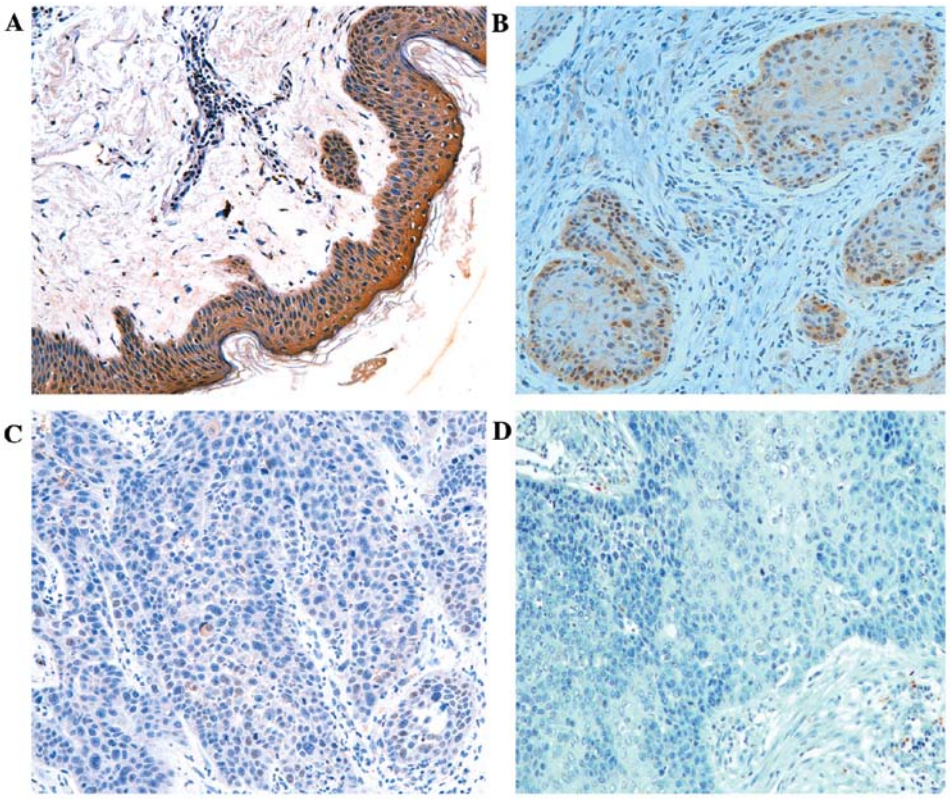

Figure 5. Immunoreaction of PFN2 protein in tissue samples. (A) Strong staining signals in paracancerous normal mucosal epithelia. (B) Moderate staining signals in cancerous tissues. (C) Low immunoreaction signals in moderately differentiated cancerous tissues. (D) Negative signals in cancerous tissues.

Table II. Expression of PFN2 in cancerous tissues and paired non-cancerous tissues.

Variables	All cases (n)	Positive expression n (%)	P-value	Expression level (n)				P-value
				None	Weak	Moderate	Strong	
Cancer	88	63 (71.6)	<0.001	25	33	28	2	<0.001
Non-cancer	88	87 (98.9)		1	18	34	35	

Immunohistochemistry analysis showed that PFN2 was expressed in the cytoplasm as well as in the nucleus. PFN2 was distributed diffusely in the cytoplasmic regions while densely in the nuclear region. Normal epithelia adjacent to the tumor showed strong reactivity to the PFN2 antibody in the cytoplasm and nucleus (Fig. 5A). Among all the cases examined, 35/88 (39.7%) paracancerous normal tissue samples demonstrated strong and positive staining of their epithelial cells, and 34/88 (38.6%) demonstrated moderate staining. As shown in Table II, only 2/88 (2.27%) of all cancerous tissues showed strong and positive expression, while 25/88 (28.4%) of all the cancerous tissues showed no staining and 33/88 (37.5%) showed weak staining (P<0.001) (Fig. 5). Statistically significant differences in the PFN2 expression was observed between cancerours and adjacent non-cancerous tissues (P<0.001) with PFN2 expression being higher in normal epithelial tissues than in malignant ones (Table II).

The relationship between decreased PFN2 expression and various clinical and histopathological features was analyzed and the results are shown in Table III. The expression levels of PFN2 was summarized as low and high expression by combining the none and the weak staining as low expression, while the moderate and the strong staining as high expression. From the statistical results shown in Table III, no significant correlation was found between PFN2 expression with age (P=0.429), gender (P=0.501), tumor location (P=0.558). Tumor size and regional lymph node metastasis were grouped according to pathological TNM staging, but no statistical difference was found in the current study. The cases were accordingly subdivided into two groups for clinical staging for further analysis: stages I+II and stages III+IV. Although PFN2 expression was heterogeneous among the different groups, the general trend of PFN2 detection can be easily identified from the statistical analysis. Of clinical stages I+II, 15/31 (51.6%) showed high expression for PFN2 compared with 15/57 (26.3%) of stages III+IV. A statistical difference was found in these groups (P=0.037). Histological groups were defined by cellular differentiation of oral squamous cancer cells within paraffin sections. The vascular invasion of cancer cells within the sections were also reviewed for correlation. A clear-cut statistical significance

Table III. Expression of PFN2 in correlation with clinicopathological variables.

Variables	No. of cases	PFN2 low[a] n (%)	PFN2 high[b] n (%)	P-value
Total	88			
Age (years)				
≤60	52	36 (69.2)	16 (30.8)	0.429
>60	36	22 (61.1)	14 (38.9)	
Gender				
Male	57	39 (68.4)	18 (31.6)	0.501
Female	31	19 (61.3)	12 (38.7)	
Tumor site				
Tongue	46	31 (67.4)	15 (32.6)	0.558
Buccal mucosa	21	12 (57.1)	9 (42.9)	
Floor of mouth	10	6 (60)	4 (40)	
Gingiva	11	9 (81.8)	2 (18.2)	
Histological grade				
Well-differentiated	35	13 (37.1)	22 (62.9)	<0.001
Moderately-differentiated	40	34 (85)	6 (15)	
Poorly-differentiated	13	11 (85.6)	2 (15.4)	
Vascular invasion				
Yes	28	25 (89.3)	3 (10.7)	<0.001
No	60	31 (51.7)	29 (48.3)	
Clinical stage				
Stages I+II	31	16 (48.4)	15 (51.6)	0.037
Stages III+IV	57	42 (73.7)	15 (26.3)	
Tumor size				
T1-2	50	30 (60)	20 (40)	0.179
T3-4	38	28 (73.7)	10 (26.3)	
Regional lymph nodes				
N0	37	22 (59.5)	15 (40.5)	0.277
N1-3	51	36 (70.6)	15 (29.4)	

[a]Expression staining score <2; [b]expression staining score >2.

Table IV. Cox regression model of overall survival for clinicopathological parameters and PFN2 expression.

	Parameter estimate	Hazard ratio	95% confidence interval	P-value
Clinical stage	0.482	1.620	1.120-2.342	<0.001
PFN2 expression	-1.255	0.285	0.184-0.441	<0.001

can be confirmed (P<0.001) for the correlation between these two pathological factors and PFN2 expression levels.

Prognostic significance of PFN2 expression from the follow-up analysis of patients with OSCC. Regarding the results of the overall survival analysis of these 88 patients, no statistically significant correlation was found for gender, age, tumor location, tumor size and regional lymph node metastasis with prognosis (Table I). On the other hand, clinical staging, histological grade, vascular invasion and PFN2 expression correlated with overall survival. The overall survival rates were 86.7% (26/30) and 29.3% (17/58), respectively, in patients with high (strong or moderate staining) and low (none or low staining) PFN2 expression. Tumors with weak PFN2 expression were associated with a significantly worse prognosis than in strongly expressed tumours (P<0.001). In addition, patients of clinical stages I+II had a longer overall survival than those of clinical stages III+IV (P=0.013). Histological differentiation

showed a strong association with survival time of the patients (P=0.004). The expected survival time was 19.8857±0.9067, 16.2750±1.0178 and 11.8462±2.0636 months for well-, moderately- and poorly-differentiated tumors, respectively. Survival curves were plotted according to the Kaplan-Meier method for the patients with PFN2 expression status and the other three afore-mentioned significant factors.

Furthermore, to evaluate the potential of PFN2 expression as an independent predictor for overall survival of HCC, multivariate Cox regression analyses were performed (Table IV). While the others failed to demonstrate independence, clinical stage and PFN2 expression level might play a role in predicting the overall survival in OSCC by showing significant prognostic predictive value to the model (P<0.001).

Discussion

OSCC is of increased concern in many countries especially in Asia due to its high incidence and poor prognosis (2,27). Although it is widely accepted that the occurrence and development of OSCC correlates with various molecular and genetic incidents, the carcinogenesis mechanism of OSCC is very complex and remains poorly understood (6). The emergence of novel comparative proteomic technologies has already facilitated the detection of potential biomarkers which are indicative of a change during the processes of cancer growth and metastasis (28). In this study, based on an *in vitro* carcinogenesis model established before, we used liquid chromatography coupled with tandem MS to identify PFN2 along with other proteins among a panel of differentially expressed proteins. Validations of several specific proteins using Western blot analysis or ELISA have been previously conducted (29-31). In the current study, we performed an *in vitro* comparison between the different cell lines by RT-PCR, real-time PCR and Western blotting and *in vivo* pathological analyses of PFN2 in OSCC cancer patients. In an attempt to analyze the relative function of the profilin family in OSCC as a whole, the largely reported PFN1, as the first profilin isoform discovered, was also studied in parallel.

The reason why in the present study the profilin family attracted so much attention, stems from the reported relationship between profilin and cytoskeleton dynamics and its interaction with a plethora of molecules such as p42POP (32), cdc42 (33), protein kinase C (PKC) (34), vasodilator-stimulated phosphoprotein (VASP) (35) and Akt (21). Profilins are actin-binding proteins which remain the driving force for cell structure changes via regulating signal-dependent actin polymerization. Actin-directed cellular changes are involved in many normal functions such as cell migration, proliferation and cytokinesis. Besides, it is well documented that the actin cytoskeleton is a central player in many carcinogenesis and cancer cell migration processes and consequently actin is involved in various aspects of cancer (36). Disruption of the actin-based cytoskeleton is a known fact following oncogene-induced cell transformation. In cells, the assembly and disassembly of actin filaments, in addition to their organization into functional 3D networks, are regulated by a variety of actin-binding proteins (ABPs). ABPs, such as cofilin (37), ACTN4 (38), gelsolin (39), cortactin (40), have frequently been observed to display genetic defect(s) in cancer cells suggesting a causal contribution to oncogenesis or malignant tumor progression. The crosstalk of profilin with different protein also instigated many studies in recent years. In 2001, Vemuri and Singh reported that profilin is phosphorylated on the C-terminal Ser137 by protein kinase C (PKC), a key enzyme of the PI3-kinase signaling pathway (34). A more recent study, identified a novel nuclear profilin-binding protein, p42POP which acts as a transcriptional repressor and whose activity is modulated by profilin binding implicating profilin in gene regulation (32).

The purpose of the present study was to unravel the potential of PFN1 or PFN2 as tumor suppressors in OSCC. PFN1 was first reported as a breast cancer tumor inhibitor several years ago by Janke *et al* (41). Since then, PFN1 has been widely reported as a potential tumor suppressor in a variety of malignant tumors, such as skin fibrosarcoma (42), pancreatic ductal adenocarcinoma (43), hepatocellular carcinoma (44) and renal carcinoma (45). The function of PFN1 has gradually been revealed in recent years as *in vitro* studies on PFN1 have now been undertaken in several breast cancer cell lines. Studies of PFN1 vector transfer, have demonstrated a reduced growth rate and improved adhesion ability in CAL51 cancer cells (41). In other studies, overexpression of PFN1 was reported to suppress motility and proliferation of cancer cells and to revert tumorigenic cells to ones with near nontumorigenic behavior, while loss of expression of PFN1 actually conferred decreased intercellular adhesion and enhanced invasiveness (46). One possible mechanism of how loss of PFN1 expression can result in increased invasiveness of breast cancer cells was believed to be through the augmentation of the PIP2 binding signal in the cellular membrane for VASP in the absence of PFN1. PFN1 and Ena/VASP proteins are in a competition for this lipid (47,48). Another interesting and noteworthy finding reported in the literature is that a functional actin-binding site is required for PFN1 to suppress cancer cell motility. This implies that the profilin-actin interaction is necessary for PFN1-induced suppression of tumor cell motility compared with the other two major PFN1 ligands (poly-proline and PIP2) (49). Overexpression of PFN1 had also been found to be correlated with increased R-cadherin expression in MDA-231 cancer cells with negative E-cadherin (50). In addition, it was revealed that overexpression of PFN1, which has been previously shown to elicit a strong antitumor effect in breast cancer cells, leads to a significant reduction in AKT phosphorylation in breast cancer cells, and this effect is mediated through PTEN up-regulation which may account for the inhibition of tumorigenicity by PFN1 overexpression (21). Although PFN1 has been studied for several years and many functions have been explored, PFN2 which retains a similar structure has not been deeply investigated for its cancer-related functions and therefore, it became the main object of the present study.

Contrary to our expectation, PFN1 mRNA levels were not found to be significantly different between the oral cancer cells and the non-tumorigenic HIOEC cells. This result was consistent with the findings at the protein level which were demonstrated by Western blotting and quantitative proteomics. The PFN2 mRNA and protein levels, which had not been previously studied in oral mucosal tissues, were demonstrated to be high in normal oral mucosal cell lines and were proven to be greatly decreased in various OSCC cell lines *in vitro*. After transfection with PFN2 vector, the proliferation of

HB96 cancer cells decreased. The growth of oral cancer cells halted because of the PFN2 effect. When comparing the immunohistochemistry staining of normal and cancerous-paired clinical tissues, we further confirmed the notion of a role of PFN2 in cancer carcinogenesis and progression and we are the first one to report this potential function.

The subcellular localization of PFN2 in normal or cancerous oral squamous cells has not been studied so far. Here, we examined the expression of PFN2 in HIOEC and two different cancer cell lines by confocal microscopy. Interestingly, the results of the confocal microscopy revealed that PFN2 localizes in both the cytoplasm and nuclear regions, implying a hypothetical role of this protein in signaling transduction in the nucleus or in nuclear structure formation and maintenance. In addition, the different expression of PFN2 in different subcellular areas was roughly compared and we found that signals from normal and tumor cells were different in intensity especially in the cytoplasm. Western blotting experiments confirmed the differences in PFN2 expression in the cytoplasm between normal and cancerous cells, while in the nucleus the amount of PFN2 expression remained fairly constant. The differences in the *in vitro* cytoplasmic expression of PFN2 between non-tumorigenic and tumorigenic cells of the oral cavity possibly reveal the role of this protein in the regulation of post-transcriptional or translational levels in cancer cells and in the altered cytostructure formation.

Immunohistochemical staining was applied to investigate the clinical implication of PFN2. The expression of PFN2 in paired cancerous and non-cancerous cells is significantly different and the down-regulation of PFN2 was widespread in OSCC tissues. This was consistent with the afore-mentioned *in vitro* results. Clinical staging was statistically correlated with the expression level of PFN2 suggesting the inhibitory function of PFN2 in cancer invasion and progression. In pathological analyses, a low PFN2 protein expression was closely correlated with a poorer cellular differentiation viewed in paraffin sections of higher malignancy. By collecting data on the overall survival of these patients, the prognostic effect of PFN2 can be concluded. Patients with tumors expressing a high level of PFN2 showed longer overall survival periods than those with negative or low levels of PFN2 expression. Combined with the *in vitro* data, it is likely that a decrease or loss of PFN2 expression could be a useful indicator for a highly malignant phenotype of oral squamous carcinoma cells.

In order to study the underlying mechanisms and the downstream signal transduction of the altered PFN2 expression in oral cancer, VASP, N-WASP and P27 were chosen to be studied. VASP is involved in the progression and invasion of several tumor cells (51). N-WASP, which is an ABP is involved in WASP-Arp2/3 complex signaling pathway and possesses many proline-rich sequences, suggesting some interaction with PFN1 and PFN2 (52). N-WASP has been confirmed as a putative breast cancer inhibitor in some studies (53). P27 is a cyclin-dependent kinase inhibitor and often causes G1 arrest of cancer cells through up-regulation of its expression levels (54). The effect of PFN1 on P27 expression has been eludicated by Zou *et al* and a causal relationship has been established on the anti-proliferative effects induced by overexpression of PFN1 (55). However in our study, P27 levels were not notably altered and N-WASP increased when PFN2 was up-regulated by transfection of the specific vector. Thus, it is conceivable that the suppressive function of PFN2 might not be associated with P27 and VASP. N-WASP has been confirmed in the study as a relevant molecule and downstream effector to PFN2 due to its cancer inhibitory effects. The cellular functions of the WASP family members, which include N-WASP, have recently been reviewed by Padrick and Rosen (56). The functions of WASP are achieved by controlling the degree, rate and location of filament nucleation by the Arp2/3 complex, which retains a central role in the control of dynamic rearrangements of the actin cytoskeleton in many cellular processes including division and movement. Both N-WASP and Arp2/3 expression have been found to be significantly correlated with the invasion and progression of different cancer types. Although the underlying mechanisms of these molecules need to be further elucidated and more research is required in this field, the PFN2-N-WASP-Arp2/3 signal transduction system may be associated with the changes we have seen in this study.

In summary, this study revealed the significant decrease of PFN2 expression in OSCC *in vitro* and *in vivo*. The subcellular localization and clinicopathological implication of PFN2 have also been assessed. Furthermore, the N-WASP-Arp2/3 signaling pathway has been proposed for the PFN2 suppressive role as observed with transfection with the expression vector. We propose that PFN2, rather than PFN1, is likely to be a candidate as a tumor suppressor in OSCC. However, more detailed downstream and upstream regulators of this protein need to be discovered to support the roles of PFN2 in OSCC proliferation, invasion and progression.

Acknowledgements

Appreciation is expressed to Dr Yan Ming for her technical assistance. This study was partially supported by the Program for Innovative Research Team of Shanghai Municipal Education Commission, and by Research Grants (10dz1951300) from the Science and Technology Commission of Shanghai Municipality, by research grants nos. 30973344 and 30700953 from the National Natural Science Foundation of China and by research grant no. 08QA14056 from the Shanghai Rising-Star Program.

References

1. Jemal A, Siegel R, Ward E, *et al*: Cancer statistics, 2006. CA Cancer J Clin 56: 106-130, 2006.
2. Chen YK, Huang HC, Lin LM and Lin CC: Primary oral squamous cell carcinoma: an analysis of 703 cases in Southern Taiwan. Oral Oncol 35: 173-179, 1999.
3. Neville BW and Day TA: Oral cancer and precancerous lesions. CA Cancer J Clin 52: 195-215, 2002.
4. Saranath D, Tandle AT, Teni TR, *et al*: p53 inactivation in chewing tobacco-induced oral cancers and leukoplakias from India. Oral Oncol 35: 242-250, 1999.
5. Kelloff GJ, Sigman CC and Contag CH: Early detection of oral neoplasia: watching with new eyes. Cancer Prev Res 2: 405-408, 2009.
6. Tsantoulis PK, Kastrinakis NG, Tourvas AD, Laskaris G and Gorgoulis VG: Advances in the biology of oral cancer. Oral Oncol 43: 523-534, 2007.
7. Aebersold R, Anderson L, Caprioli R, Druker B, Hartwell L and Smith R: Perspective: a program to improve protein biomarker discovery for cancer. J Proteome Res 4: 1104-1109, 2005.
8. Al-Shahib A, Misra R, Ahmod N, Fang M, Shah H and Gharbia S: Coherent pipeline for biomarker discovery using mass spectrometry and bioinformatics. BMC Bioinformatics 11: 437, 2010.

9. Diamandis EP: Mass spectrometry as a diagnostic and a cancer biomarker discovery tool: opportunities and potential limitations. Mol Cell Proteomics 3: 367-378, 2004.
10. Iwadate Y: Clinical proteomics in cancer research-promises and limitations of current two-dimensional gel electrophoresis. Curr Med Chem 15: 2393-2400, 2008.
11. El Yazidi-Belkoura I, Adriaenssens E, Vercoutter-Edouart AS, Lemoine J, Nurcombe V and Hondermarck H: Proteomics of breast cancer: outcomes and prospects. Technol Cancer Res Treat 1: 287-296, 2006.
12. Granville CA and Dennis PA: An overview of lung cancer genomics and proteomics. Am J Respir Cell Mol Biol 32: 169-176, 2005.
13. Mazzanti R, Solazzo M, Fantappié O, *et al*: Differential expression proteomics of human colon cancer. Am J Physiol Gastrointest Liver Physiol 290: G1329-G1338, 2006.
14. Sun Y, Mi W, Cai J, *et al*: Quantitative proteomic signature of liver cancer cells: tissue transglutaminase 2 could be a novel protein candidate of human hepatocellular carcinoma. J Proteome Res 7: 3847-3859, 2008.
15. Uribe R and Jay D: Review of actin binding proteins: new perspectives. Mol Biol Rep 36: 121-125, 2009.
16. Schlüter K, Jockusch BM and Rothkegel M: Profilins as regulators of actin dynamics. Biochim Biophys Acta 1359: 97-109, 1997.
17. Didry D, Carlier MF and Pantaloni D: Synergy between actin depolymerizing factor cofilin and profilin in increasing actin filament turnover. J Biol Chem 273: 25602-25611, 1998.
18. Wegner A: Head to tail polymerization of actin. J Mol Biol 108: 139-150, 1976.
19. Bubb MR, Yarmola EG, Gibson BG and Southwick FS: Depolymerization of actin filaments by profilin. Effects of profilin on capping protein function. J Biol Chem 278: 24629-24635, 2003.
20. Pilo Boyl P, Di Nardo A, Mulle C, *et al*: Profilin 2 contributes to synaptic vesicle exocytosis, neuronal excitability, and novelty-seeking behavior. EMBO J 26: 2991-3002, 2007.
21. Das T, Bae YH, Wells A and Roy P: Profilin-1 overexpression upregulates PTEN and suppresses AKT activation in breast cancer cells. J Cell Physiol 218: 436-443, 2009.
22. Sdek P, Zhang ZY, Cao J, *et al*: Alteration of cell-cycle regulatory proteins in human oral epithelial cells immortalized by HPV16 E6 and E7. Int J Oral Maxillofac Surg 35: 653-657, 2006.
23. Zhong LP, Pan HY, Zhou XJ, *et al*: Characteristics of a cancerous cell line, HIOEC-B(a)P-96, induced by benzo(a)pyrene from human immortalized oral epithelial cell line. Arch Oral Biol 53: 443-452, 2008.
24. Pan HY, Zhang ZY, Zhou XJ, Li J, He RG and Chen WT: The establishment of a carcinogenesis model of oral squamous cell carcinoma in vitro. Zhonghua Kou Qiang Yi Xue Za Zhi 41: 20-24, 2006.
25. Dong Z, Wei F, Zhou C, *et al*: Silencing Id-1 inhibits lymphangiogenesis through down-regulation of VEGF-C in oral squamous cell carcinoma. Oral Oncol 47: 27-32, 2010.
26. Wei KJ, Zhang L, Yang X, *et al*: Overexpression of cytokeratin 17 protein in oral squamous cell carcinoma in vitro and in vivo. Oral Dis 15: 111-117, 2009.
27. Subapriya R, Thangavelu A, Mathavan B, Ramachandran CR and Nagini S: Assessment of risk factors for oral squamous cell carcinoma in Chidambaram, Southern India: a case-control study. Eur J Cancer Prev 16: 251-256, 2007.
28. Wulfkuhle JD, Liotta LA and Petricoin EF: Proteomic applications for the early detection of cancer. Nat Rev Cancer 3: 267-275, 2003.
29. Yang X, Wei KJ, Zhang L, *et al*: Increased expression of Cathepsin B in oral squamous cell carcinoma. Int J Oral Maxillofac Surg 39: 174-181, 2010.
30. Zhang L, Yang X, Pan HY, *et al*: Expression of growth differentiation factor 15 is positively correlated with histopathological malignant grade and in vitro cell proliferation in oral squamous cell carcinoma. Oral Oncol 45: 627-632, 2008.
31. Zhang L, Wei KJ, Yang X, *et al*: Overexpression of Galectin-1 is negatively correlated with pathologic differentiation grade in oral squamous cell carcinoma. J Cancer Res Clin Oncol 136: 1527-1535, 2010.
32. Birbach A, Verkuyl JM and Matus A: Reversible, activity-dependent targeting of profilin to neuronal nuclei. Exp Cell Res 312: 2279-2287, 2006.
33. Yang C, Huang M, DeBiasio J, *et al*: Profilin enhances Cdc42-induced nucleation of actin polymerization. J Cell Biol 150: 1001-1012, 2000.
34. Vemuri B and Singh SS: Protein kinase C isozyme-specific phosphorylation of profilin. Cell Signal 13: 433-439, 2001.
35. Quinlan MP: Vinculin, VASP, and profilin are coordinately regulated during actin remodeling in epithelial cells, which requires de novo protein synthesis and protein kinase signal transduction pathways. J Cell Physiol 200: 277-290, 2004.
36. Lambrechts A, Van Troys M and Ampe C: The actin cytoskeleton in normal and pathological cell motility. Int J Biochem Cell Biol 36: 1890-1909, 2004.
37. Wang W, Eddy R and Condeelis J: The cofilin pathway in breast cancer invasion and metastasis. Nat Rev Cancer 7: 429-440, 2007.
38. Khurana S, Chakraborty S, Cheng X, Su YT and Kao HY: The actin-binding protein, actinin alpha 4 (ACTN4), is a nuclear receptor coactivator that promotes proliferation of MCF-7 breast cancer cells. J Biol Chem 286: 1850-1859, 2011.
39. Van den Abbeele A, De Corte V, Van Impe K, *et al*: Down-regulation of gelsolin family proteins counteracts cancer cell invasion in vitro. Cancer Lett 255: 57-70, 2007.
40. Jia L, Uekita T and Sakai R: Hyperphosphorylated cortactin in cancer cells plays an inhibitory role in cell motility. Mol Cancer Res 6: 654-662, 2008.
41. Janke J, Schlüter K, Jandrig B, *et al*: Suppression of tumorigenicity in breast cancer cells by the microfilament protein profilin 1. J Exp Med 191: 1675-1686, 2000.
42. Shi Y, Elmets CA, Smith JW, *et al*: Quantitative proteomes and in vivo secretomes of progressive and regressive UV-induced fibrosarcoma tumor cells: mimicking tumor microenvironment using a dermis-based cell-trapped system linked to tissue chamber. Proteomics 7: 4589-4600, 2007.
43. Cecconi D, Astner H, Donadelli M, *et al*: Proteomic analysis of pancreatic ductal carcinoma cells treated with 5-aza-2'-deoxycytidine. Electrophoresis 24: 4291-4303, 2003.
44. Wu N, Zhang W, Yang Y, *et al*: Profilin 1 obtained by proteomic analysis in all-trans retinoic acid-treated hepatocarcinoma cell lines is involved in inhibition of cell proliferation and migration. Proteomics 6: 6095-6106, 2006.
45. Minamida S, Iwamura M, Kodera Y, *et al*: Profilin 1 overexpression in renal cell carcinoma. Int J Urol 18: 63-71, 2011.
46. Roy P and Jacobson K: Overexpression of profilin reduces the migration of invasive breast cancer cells. Cell Motil Cytoskeleton 57: 84-95, 2004.
47. Ding Z, Lambrechts A, Parepally M and Roy P: Silencing profilin-1 inhibits endothelial cell proliferation, migration and cord morphogenesis. J Cell Sci 119: 4127-4137, 2006.
48. Bae YH, Ding Z, Zou L, Wells A, Gertler F and Roy P: Loss of profilin-1 expression enhances breast cancer cell motility by Ena/VASP proteins. J Cell Physiol 219: 354-364, 2009.
49. Wittenmayer N, Jandrig B, Rothkegel M, *et al*: Tumor suppressor activity of profilin requires a functional actin binding site. Mol Biol Cell 15: 1600-1608, 2004.
50. Zou L, Hazan R and Roy P: Profilin-1 overexpression restores adherens junctions in MDA-MB-231 breast cancer cells in R-cadherin-dependent manner. Cell Motil Cytoskeleton 66: 1048-1056, 2009.
51. Kwiatkowski AV, Gertler FB and Loureiro JJ: Function and regulation of Ena/VASP proteins. Trends Cell Biol 13: 386-392, 2003.
52. Rohatgi R, Ma L, Miki H, *et al*: The interaction between N-WASP and the Arp2/3 complex links Cdc42-dependent signals to actin assembly. Cell 97: 221-231, 1999.
53. Sanchez AM, Flamini MI, Baldacci C, Goglia L, Genazzani AR and Simoncini T: Estrogen receptor-(alpha) promotes breast cancer cell motility and invasion via focal adhesion kinase and N-WASP. Mol Endocrinol 24: 2114-2125, 2010.
54. Liu S and Yamauchi H: p27-associated G1 arrest induced by hinokitiol in human malignant melanoma cells is mediated via down-regulation of pRb, Skp2 ubiquitin ligase, and impairment of Cdk2 function. Cancer Lett 286: 240-249, 2009.
55. Zou L, Ding Z and Roy P: Profilin-1 overexpression inhibits proliferation of MDA-MB-231 breast cancer cells partly through p27kip1 upregulation. J Cell Physiol 223: 623-629, 2010.
56. Padrick SB and Rosen MK: Physical mechanisms of signal integration by WASP family proteins. Annu Rev Biochem 79: 707-735, 2010.